Scattering as a tool to study nuclear structure toward the drip lines

S. Karataglidis[a] and K. Amos[b]

[a] Department of Physics and Electronics, Rhodes University Grahamstown, 6140, South Africa

[b] School of Physics, University of Melbourne, Victoria, 3010, Australia

Abstract

Results are presented for the elastic scattering of electrons and protons from the exotic He and Li isotopes. Comparison with scattering results from the stable He and Li nuclei allows for an investigation into the effects that the extensive neutron distributions have on the charge density. For comparison we also consider the proton halo nucleus ^{8}B. The consequences and possible suggestions for proposed electron scattering facilities for exotic nuclei are discussed.

I. INTRODUCTION

Current microscopic understanding of structures of exotic nuclei, both of halo and skin type, has been made possible by their use in analysis of data from the elastic and inelastic scattering of those nuclei from hydrogen. In inverse kinematics such data equate to elastic and inelastic proton scattering and so one is able to probe the matter densities of such systems. As the pn component of the nucleon-nucleon (NN) force is dominant at intermediate energies [1], proton scattering primarily probes the neutron density and vice-versa. As an example, the neutron halo in ^{6}He was clearly established by analyses of ^{6}He-p scattering data [2, 3]. To do so requires use of predictive models of nucleon-nucleus (NA) scattering which are sensitive to the details of the matter density. One such is the Melbourne model [1] which has been successful in predicting observables for many elastic and inelastic NA scatterings.

But analyses of pA scattering data from exotic neutron-rich systems generally do not allow for the direct investigation of their proton densities. With the development of electron-ion colliders, and the more novel approach of constructing Self-Confining Radioactive Ion Targets (SCRIT), the possibility now exists for the direct investigation of the charge density of exotic halo and skin nuclei by electron scattering. (For both developments, see the review by Suda and Wakasugi [4].) Additionally, kinematic reconstruction of events from those facilities will provide measurements of both longitudinal and transverse form factors. Such will probe both the charge and current densities of the exotic nuclei, complementing the information on the matter densities provided by modern NA scattering analyses [1].

Taken together, a complete map of exotic nuclei will be possible. The purposes of this paper is to consider both proton and electron scattering from exotic nuclei to identify effects of the halo, or skin, in data from complementary experiments. Further, by comparing also to analyses of data from stable nuclei, one may consider how the densities change with the addition of protons or neutrons as one approaches the drip lines.

In the next three sections, outlines are given of the microscopic models we use to evaluate proton and electron scattering observables. Then, results are presented for scattering from the He and Li isotopes, concluding with ^{8}B, after which follow our conclusions.

1

II. INTERMEDIATE ENERGY NUCLEON SCATTERING

A prerequisite for the use of proton scattering data as an analysis tool for nuclear structure is a model which is able to predict scattering observables without any *a posteriori* adjustments of parameters. Such a model is that using the Melbourne force, when all nuclear structure and scattering details are preset. With this prescription, elastic scattering differential cross section and spin observable data have been well reproduced. The full model is described in a review [1] from which a brief overview follows.

To describe intermediate energy NA data one begins with a credible effective NN force. In general, such should link to the NN g matrices, which we take to be solutions of the Brueckner-Bethe-Goldstone (BBG) equations for infinite nuclear matter, *viz.*

$$g\left(\mathbf{q}', \mathbf{q}; K\right) = V\left(\mathbf{q}', \mathbf{q}\right) + \int V\left(\mathbf{q}', \mathbf{k}'\right) \frac{Q\left(\mathbf{k}', \mathbf{K}; k_f\right)}{\left[E\left(\mathbf{k}, \mathbf{K}\right) - E\left(\mathbf{k}', \mathbf{K}\right)\right]} g\left(\mathbf{k}', \mathbf{q}; K\right) d\mathbf{k}', \qquad (1)$$

where Q is a Pauli blocking operator, and medium effects are incorporated into the auxiliary potentials entering the energy denominator [1]. The center-of-mass and Fermi momenta are denoted by K and k_f, respectively.

The BBG g matrices are mapped to a usable coordinate space form of complex, energy and density dependent, model NN effective interaction (g_{eff}), which when folded with any microscopic model structure of the target gives the NA optical potential of the form,

$$U\left(\mathbf{r}, \mathbf{r}'; E\right) = \delta\left(\mathbf{r} - \mathbf{r}'\right) \sum_i n_i \int \varphi_i^*(\mathbf{s}) g_D\left(\mathbf{r}, \mathbf{s}; E\right) \varphi_i(\mathbf{s}) \, d\mathbf{s} + \sum_i n_i \varphi_i^*(\mathbf{r}) g_E\left(\mathbf{r}, \mathbf{r}'; E\right) \varphi_i(\mathbf{r}')$$

$$= U_D\left(\mathbf{r}; E\right) \delta\left(\mathbf{r} - \mathbf{r}'\right) + U_E\left(\mathbf{r}, \mathbf{r}'; E\right), \qquad (2)$$

where the subscripts D, E denote the direct and exchange parts of the optical potential, respectively. The sums are taken over the bound state single-particle orbits for which n_i are the associated occupation numbers. In evaluations with the DWBA98 code [5], the single-particle wave functions may be taken as either of harmonic oscillator (HO) or Woods-Saxon (WS) form. A variant code now has been developed to use Skyrme-Hartree-Fock wave functions. The resultant complex, energy and density-dependent (g-folding) optical potential so formed, contains central and spin-orbit terms. With such generated in the DWBA98 code [5], they are then used to calculate differential cross sections and spin-dependent observables. They are also used in that code to evaluate cross sections and the like for inelastic scattering with the self same g_{eff} being taken as the transition operator. That inelastic scattering is calculated in the distorted wave approximation (DWA). For this the transition amplitude may be written as

$$T_{J_f J_i}^{M_f M_i \nu' \nu}(\theta) = \left\langle \chi_{\nu'}^{(-)} \right| \left\langle \Psi_{J_f M_f} \right| A g_{\text{eff}}(0, 1) \mathcal{A}_{01} \left\{ \left| \chi_\nu^{(+)} \right\rangle \left| \Psi_{J_i M_i} \right\rangle \right\}, \qquad (3)$$

where $\chi^{(\pm)}$ denoted the distorted wave functions for an incoming/outgoing nucleon, respectively, and 0,1 denote the coordinates of the projectile and bound state nucleon, respectively.

A co-factor expansion of the many-body bound-state wave function [1] leads to,

$$T_{J_f J_i}^{M_f M_i \nu' \nu}(\theta) = \sum_{\alpha_1 \alpha_2 m_1 m_2} \sum_{JM} \frac{(-1)^{j_1 - m_1}}{\sqrt{2J_f + 1}} \langle j_2 \, m_2 \, j_1 \, -m_1 | J_f \, M_f \rangle \langle J_i \, M_i \, J \, M \, | \, J_f \, M_f \rangle$$
$$\times \left\langle J_f \left\| \left[a_{\alpha_2}^\dagger \times \tilde{a}_{\alpha_1} \right]^J \right\| J_i \right\rangle$$
$$\times \left\langle \chi_{\nu'}^{(-)}(0) \right| \langle \varphi_{\alpha_2}(1) | A g_{\text{eff}}(0,1) \mathcal{A}_{01} \left\{ \left| \chi_\nu^{(+)}(0) \right\rangle | \varphi_{\alpha_1}(1) \rangle \right\} \quad (4)$$

for an angular momentum transfer J. In this equation, α designates the set of single-particle quantum numbers $\{n, l, j, m_\tau\}$, where τ is the nucleon isospin.

III.   ELECTRON SCATTERING

The approach we adopt for the calculation of longitudinal and transverse form factors follows that of deForest and Walecka [6], and of Karataglidis, Halse, and Amos [7]. A brief summary is given herein.

Form factors for electron scattering between nuclear states J_i and J_f involving angular momentum transfer J may be expressed as

$$|F_J^\eta(q)|^2 = \frac{1}{2J_i + 1} \left(\frac{4\pi}{Z^2} \right) |\langle J_f \| T_J^\eta(q) \| J_i \rangle|^2, \quad (5)$$

where η selects the longitudinal, transverse electric, or transverse magnetic form factors. Assuming one-body operators, the reduced matrix elements may be expressed in the form

$$\langle J_f \| T_J^\eta(q) \| J_i \rangle = \text{Tr}\,(SM)\,/\sqrt{2J + 1}, \quad (6)$$

where S is the matrix of one-body transition densities and M contains the single-particle matrix elements of the one-body longitudinal or transverse electromagnetic operators. Bare operators are used for the results presented herein, and explicit meson-exchange-current (MEC) effects are ignored. However, MEC have been incorporated implicitly in the transverse electric form factors in the long-wavelength limit by using Siegert's theorem [8].

IV.   NUCLEAR STRUCTURE

The nuclear structure information entering in analyses of both nucleon and electron scattering data are the one-body density matrix elements (OBDME), $S_{\alpha_1 \alpha_2 J}$ *viz.*

$$S_{\alpha_1 \alpha_2 J} = \left\langle J_f \left\| \left[a_{\alpha_2}^\dagger \times \tilde{a}_{\alpha_1} \right]^J \right\| J_i \right\rangle. \quad (7)$$

For elastic scattering these reduce essentially to the nucleon occupation numbers, and we have used the shell model to obtain them.

One also requires specification of the single-particle bound-state wave functions, for which we have used both HO and WS wave functions. In the case of scattering from halo nuclei, the former gives the "nonhalo" results while results from use of the latter are denoted "halo" when the binding energies of the valence orbits are set to the single-particle separation energy.
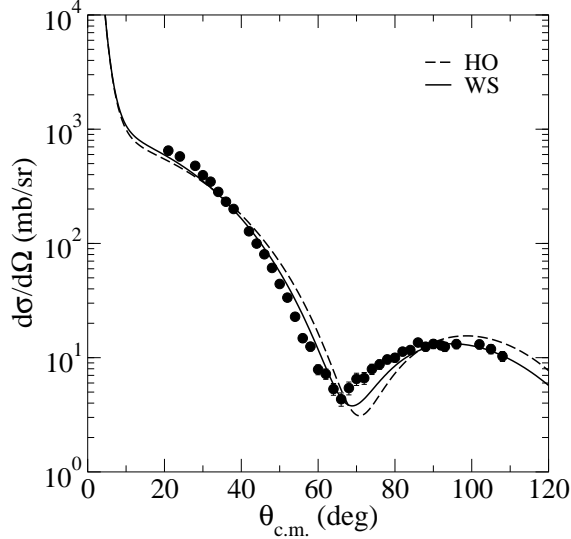
3

FIG. 1: Comparison of predictions for the differential cross section for the elastic scattering of $16A$ MeV ^{8}He ions from hydrogen. The data are those of Skaza *et al.* [10].

V. RESULTS

We first consider elastic and inelastic intermediate energy proton scattering. It has been established in ^{6}He-hydrogen scattering at $41A$ MeV [2] that ^{6}He has a neutron halo, and this was subsequently confirmed in analyses of data taken at $25A$ MeV [3]. Those were made using the WS functions defined in Ref. [9] for the specification of the halo. New data are available for the elastic scattering of ^{8}He from hydrogen at $16A$ MeV [10]. A complete $(0 + 2 + 4)\hbar\omega$ shell model with the Zheng G matrix interaction [11] was used with the WS functions of Ref. [9] but without the shallow binding for the halo neutrons in ^{6}He. Comparison of our prediction with those data is presented in Fig. 1. The similarity between the results obtained using the HO and WS single-particle wave functions confirms that ^{8}He does not have a neutron halo but rather it has a neutron skin. Our results may be compared with those presented in Ref. [10], which used the JLM effective interaction together with an explicit coupling to the (p, d) channel with ^{7}He as an intermediate state. That particular model is most problematic: ^{7}He may not be treated as an intermediate state in elastic scattering as that nucleus is particle unstable. It will break up immediately $(\tau_{1/2} = 2.2 \times 10^{-21}$ s [12]) and so the probability of the reformation of ^{8}He from ^{7}He+d is negligible. Use of that model required an unreasonably low normalization $(\lambda_W = 0.2)$ of the imaginary part of the optical potential [10] to obtain agreement with the data.

Data have also been obtained recently for elastic and inelastic scattering of ^{10}C and ^{11}C from hydrogen [13], at $45A$ and $40A$ MeV, respectively. We have analyzed those data using densities obtained from a complete $(0 + 2)\hbar\omega$ shell model using the MK3W [14] and WBT [15] interactions. Our results are compared with the available data in Figs. 2(a) and 2(b). HO wave functions with $b = 1.6$ fm were used to obtain both sets of results. The data for the elastic scattering from both nuclei are well reproduced, indicating that the structure model suffices to specify the ground state densities of ^{10,11}C. The result for elastic scattering of ^{10}C using the WBT interaction is not shown as it is very similar to that found using the MK3W. Note that no adjustment of the input potentials or wave functions have been made
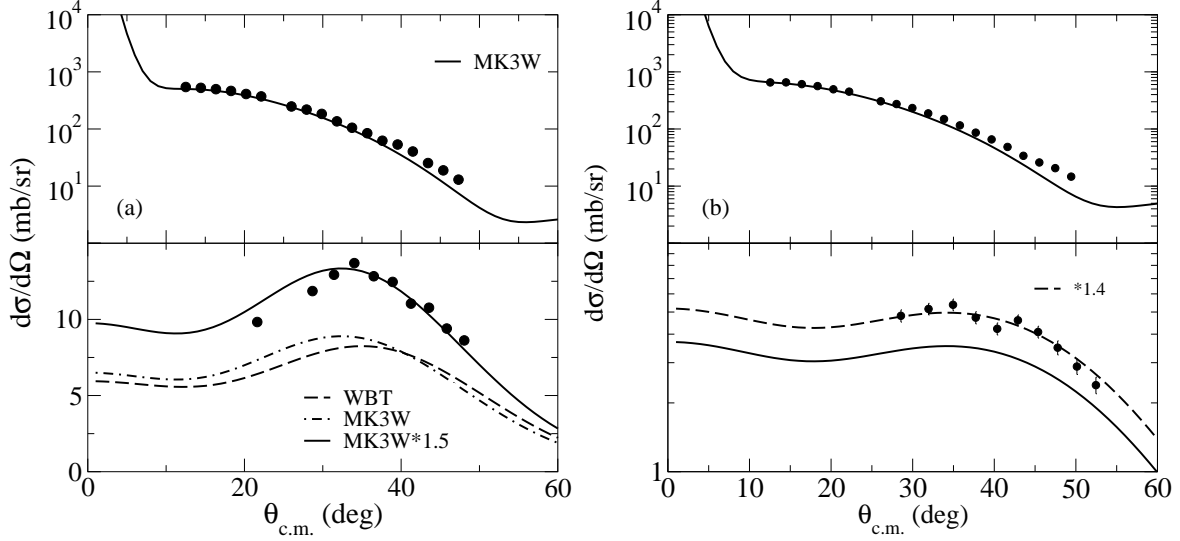
4

FIG. 2: ^{10}C (a) and ^{11}C (b) scattering from hydrogen at $45A$ and $40A$ MeV, respectively. The top part of the panels show the elastic scattering while the bottom panels show the inelastic scattering as described in the text. The data are from Ref. [13].

in obtaining these results. As with the case of ^{8}He$+p$ scattering, this is in contrast to the earlier JLM calculations which required a renormalization of the *real* part of the potential by $\sim 10\%$, an adjustment for which there is no *a priori* reason, other than it appears to be a general trend. This is more a serious problem with the underlying JLM potential. A more drastic renormalization is required with that model to describe the data for the elastic scattering from ^{6}He [13] as well.

The data for the inelastic scattering to the 2^+ state in ^{10}C and $\frac{5}{2}^-$ state in ^{11}C are shown in the bottom panels of Figs. 2(a) and 2(b), respectively. In each case, the results of our calculations underestimate the data, both requiring a renormalization of around 1.4 to obtain agreement. But in both cases the shape is reproduced very well. This indicates that some additional core polarization terms are missing in the structure model. Higher-order $\hbar\omega$ components in the model space are needed as studies of $p - {}^{12}$C scattering [1] showed them to be for evaluation of the 2^+ (4.43 MeV) state excitation.

The longitudinal elastic electron scattering form factors for ^{4,6,8}He are displayed in Fig. 3. The comparison of the ^{4}He form factor with the available data is quite good up to 2.5 fm^{-1}. This is consistent with the predicted charge radius of 1.71 fm, as compared to the measured value of 1.671 ± 0.014 fm [17]. The form factors for ^{6}He and ^{8}He have been calculated using WS functions as used in the analysis of proton scattering. The addition of neutrons to form ^{6}He and ^{8}He pull the charge density out and thus the form factors decrease with momentum transfer. Note that the detailed properties of the neutron halo in ^{6}He do not affect the form factor; it is only the presence of the extra 2 neutrons that causes the change to the proton distribution.

The longitudinal and transverse elastic electron scattering form factors for ^{7}Li, ^{9}Li and ^{11}Li are displayed in Figs. 4(a) and 4(b), respectively. The level of agreement between the results of our calculations for ^{7}Li with data [18, 19, 20] is quite good. The addition of two neutrons does not change the form factors substantially and so the charge density for ^{9}Li is little changed from that for ^{7}Li. But a noticeable change is observed in the form factors
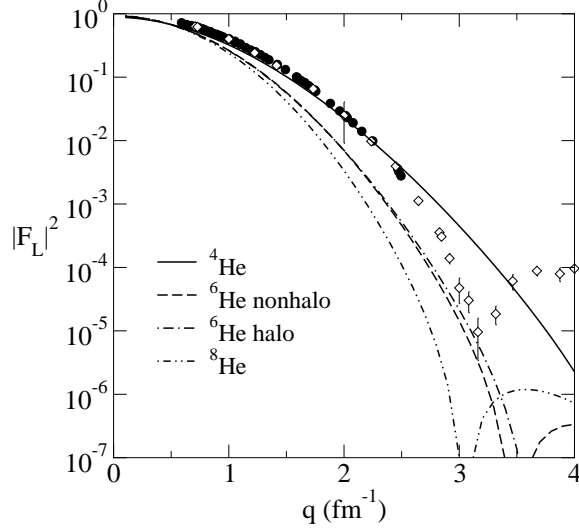
FIG. 3: Elastic electron scattering form factors for ^{4,6,8}He. The data for the ^{4}He form factor are those of McCarthy *et al.* [16].

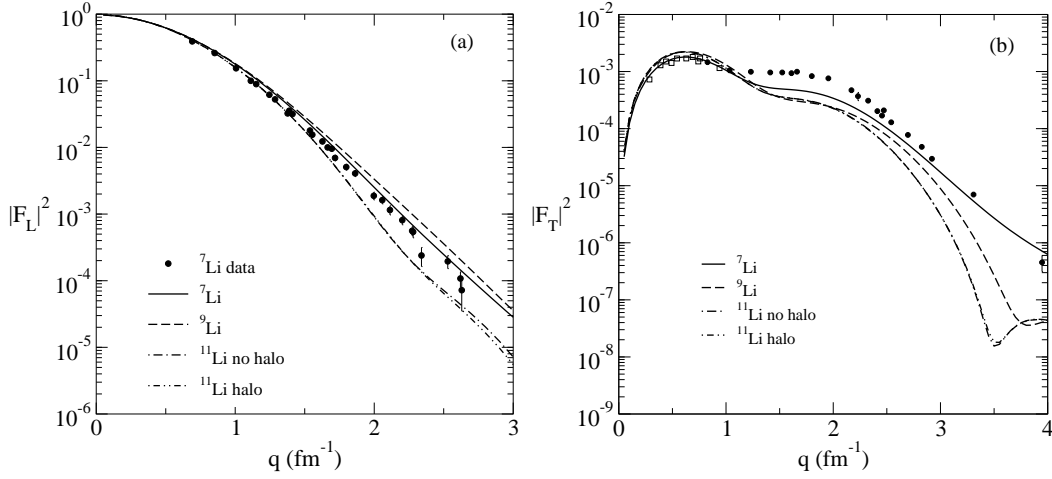FIG. 4: Longitudinal (a) and transverse (b) form factors for ^{7}Li, ^{9}Li, and ^{11}Li. The data are from Refs. [18, 19, 20].

for ^{11}Li, evidenced by the longitudinal form factor decreasing with momentum transfer. As with ^{6}He, this change does not come about with the halo specifics in this nucleus; rather, it is due only to the coupling of the 4 extra neutrons to the ^{7}Li core.

As a comparison to the neutron halos, we now turn our attention to the scattering from a proton halo nucleus, namely ^{8}B. A complete $(0 + 2 + 4)\hbar\omega$ shell model using the Zheng interaction [11] was used to obtain the OBDME. The single proton separation energy from ^{8}B is 137 keV [21] and we use WS functions with that binding energy to specify the halo. The non-halo specification uses the same set of WS functions as for ^{8}He. Our prediction of the differential cross section for the elastic scattering of 65 MeV protons from ^{8}B is shown in Fig. 5. As for ^{6}He and ^{11}Li, the halo manifests itself as a reduction in the cross section at large angles. This is due to a reduction of the proton density at the core, a consequence of requiring the density to extend out to large radius while preserving particle number.
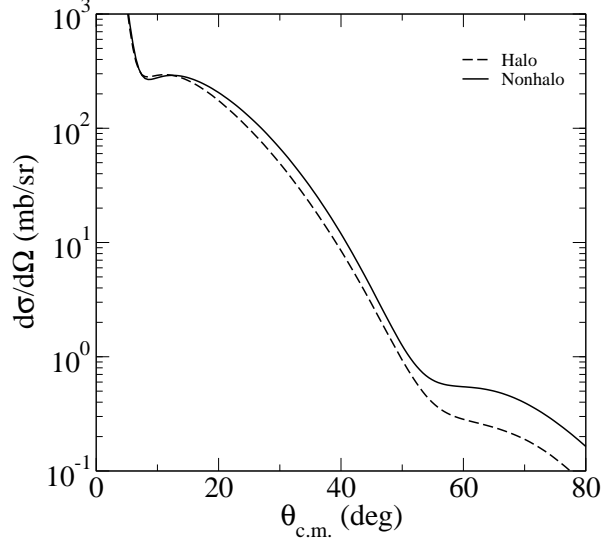
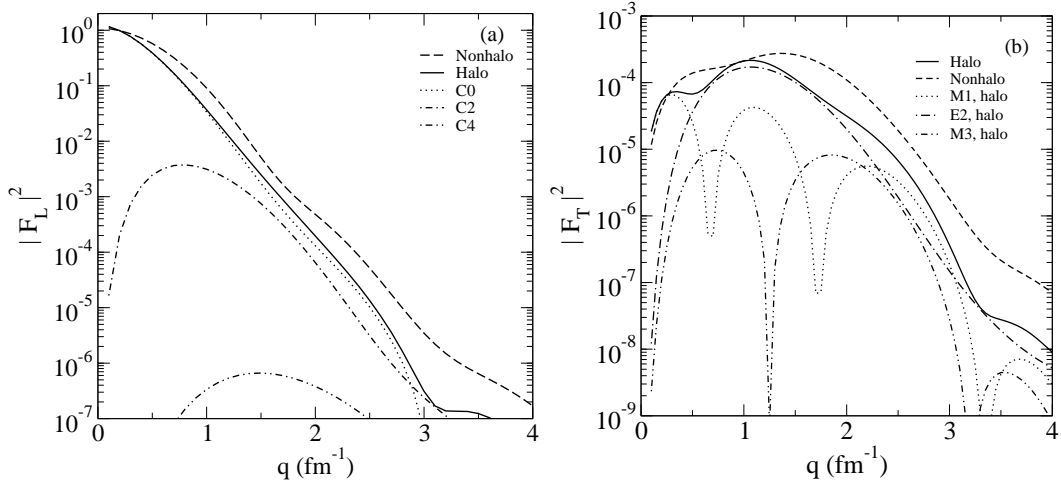FIG. 5: Differential cross section predictions for the elastic scattering of 65 MeV protons from ^{8}B.

FIG. 6: Longitudinal (a) and transverse (b) elastic electron scattering form factors for ^{8}B.

Our predictions for the longitudinal and transverse elastic electron scattering form factors are shown in Figs. 6(a) and 6(b). The longitudinal form factor is dominated by the $C0$ component below 1 fm^{-1} while the $C2$ contribution becomes significant above that value of momentum transfer. The $C4$ component is negligible. The effects of the proton halo, in this case, is distinct. Notably, the form factor decreases with momentum transfer which is consistent with a more extensive charge distribution. That effect is also noticeable in the transverse form factor, Fig. 6(b), which is dominated by the $E2$ component. Thus, the halo also affects the current density as that is related to the charge density through the continuity equation.

VI. CONCLUSIONS

We have presented results for the elastic scattering of protons and electrons from exotic nuclei, including halo systems, in order to elicit details of the effects of the extended nucleon matter on the charge density. While proton scattering is sensitive to the details of the neutron halo, it has been shown, in the longitudinal electron scattering form factors of ^{6}He and ^{11}Li, that the neutron halo does not affect the charge density. Instead the charge density is extended naturally only through the addition of neutrons to the stable isotopes. That will occur irrespective of whether the exotic nucleus is a neutron halo or a skin. The transverse form factors of the neutron-rich systems portray similar effects where the change to the current density is due simply to the addition of neutrons and not specifically if they form a neutron halo or skin.

The situation for proton halos is entirely different. The longitudinal and transverse electron scattering form factors for ^{8}B are significantly reduced. This is consistent with the extension of the charge density due to the proton halo. The transverse form factor is dominated by the $E2$ term which is also affected by the proton halo.

With the introduction of the electron-ion collider, it is hoped that investigations of the proton halos will be possible. Transverse form factors should also be measured as such measurements will also be possible in the colliders. Analysis with complementary proton scattering data will allow for the possibility of the complete mapping the densities of exotic nuclei allowing for more detailed microscopic tests of structure models in use.

[1] K. Amos, P. J. Dortmans, H. V. von Geramb, S. Karataglidis, and J. Raynal, Adv. in Nucl. Phys. **25**, 275 (2000), and referencees cited therein.

[2] A. Lagoyannis et al., Phys. Lett. **B518**, 27 (2001).

[3] S. Stepantsov et al., Phys. Lett. **542B**, 35 (2002).

[4] T. Suda and M. Wakasugi, Prog. Part. Nucl. Phys. **55**, 417 (2005).

[5] J. Raynal, *Computer Program DWBA98, NEA 1209/05* (1998).

[6] T. deForest and J. D. Walecka, Adv. Phys. **15**, 1 (1966).

[7] S. Karataglidis, P. Halse, and K. Amos, Phys. Rev. C **51**, 2494 (1995).

[8] J. L. Friar and W. C. Haxton, Phys. Rev. C **31**, 2027 (1985).

[9] S. Karataglidis, P. J. Dortmans, K. Amos, and C. Bennhold, Phys. Rev. C **61**, 024319 (2000).

[10] F. Skaza et al., Phys. Lett. **B619**, 82 (2005).

[11] D. C. Zheng, B. R. Barrett, J. P. Vary, W. C. Haxton, and C.-L. Song, Phys. Rev. C **52**, 2498 (1995).

[12] D. R. Tilley, C. M. Cheves, J. L. Godwin, G. M. Hale, H. M. Hofmann, J. H. Kelly, C. G. Sheu, and H. R. Weller, Nucl. Phys. **A708**, 3 (2002).

[13] C. Jouanne et al., Phys. Rev. C **72**, 014308 (2005).

[14] E. K. Warburton and D. J. Millener, Phys. Rev. C **39**, 1120 (1989).

[15] E. K. Warburton and B. A. Brown, Phys. Rev. C **46**, 923 (1992).

[16] J. S. McCarthy, I. Sick, and R. R. Whitney, Phys. Rev. C **15**, 1396 (1977).

[17] C. R. Ottermann, G. Köbschall, K. Maurer, K. Rörich, C. Schmitt, and V. H. Walter, Nucl. Phys. **A436**, 688 (1985).

[18] L. R. Suelzle, M. R. Yearian, and H. Crannell, Phys. Rev. **162**, 992 (1967).

[19] J. Lichtenstadt, J. Alster, M. A. Moinester, J. Dubach, R. S. Hicks, G. A. Peterson, and S. Kowlaski, Phys. Lett. **B219**, 394 (1989).

[20] G. J. C. van Niftrik, L. Lapikás, H. de Vries, and G. Box, Nucl. Phys. **A174**, 173 (1971).

[21] D. R. Tilley, J. H. Kelley, J. L. Godwin, D. J. Millener, J. E. Purcell, C. G. Sheu, and H. R. Weller, Nucl. Phys. **A745**, 155 (2004).